

The nature of self-localization of Bose-Einstein condensates in deep optical lattices

Holger Hennig¹, Ragnar Fleischmann²

¹*Department of Physics, Harvard University, Cambridge, MA 02138, USA and*

²*Max Planck Institute for Dynamics and Self-Organization, 37073 Göttingen, Germany*

We analyze the nature of a novel type of self-trapping transition called self-localization (SL) of Bose-Einstein condensates in one-dimensional optical lattices in the presence of weak local dissipation. SL has recently been observed in several studies based upon the discrete nonlinear Schrödinger equation (DNLS), however, its origin is hitherto an open question. We show that SL is based upon a self-trapping crossover in the system. Furthermore, we establish that the origin of the crossover is the Peierls-Nabarro barrier, an energy threshold describing the stability of self-trapped states. Beyond the mean-field description the crossover becomes even sharper which is also reflected by a sudden change of the coherence of the condensate. While we expect that the crossover can be readily studied in current experiments in deep optical lattices, our results allow for the preparation of robust and long-time coherent quantum states.

PACS numbers: 03.75.Lm, 03.65.Yz, 03.75.Gg, 63.20.Pw

I. INTRODUCTION

Dissipation is typically known to represent a major obstacle in the coherent control of quantum systems. However, in recent years, a strong interest in engineered dissipation has evolved, where dissipation has been used as a tool for quantum state preparation [1, 2] as well as quantum information processing and entanglement generation [3] and to induce self-trapping (ST) [4–7]. Bose-Einstein condensates (BECs) have been shown to support a variety of different kinds of ST, both in the continuous case (such as bright and dark solitons [8–13]) and in discrete systems [14–22]. A particularly high level of control has been achieved in a two-mode BEC [15], where ST can also be induced by local dissipation which can even repurify a BEC [23].

A novel self-trapping transition coined ‘self-localization’ has been observed numerically in several studies based upon the DNLS in the presence of weak boundary dissipation in one-dimensional deep optical lattices [24–27]. In contrast to self-trapping, where a system is either prepared in a self-trapped state [14, 15, 28] or driven towards it [4, 6, 7], SL is a mechanism where in presence of weak local or boundary dissipation a very general initially diffusive state leads to the formation of one or more discrete breathers (DBs, see [29, 30] for an overview). However, SL was only found, if the atomic interaction strength exceeds a critical value [26]. While the phenomenology of SL has been studied, the mechanisms that lead to this transition have remained unknown up to now.

In this letter, we propose a mechanism for SL allowing us to give an explicit formula for an upper bound estimate of the SL threshold for the DNLS in excellent agreement with the numerical findings of [26]. The mechanism is based on a ‘crossover’ which surprisingly becomes much sharper when quantum corrections beyond the mean-field description are included, which is observed, e.g., in the condensate fraction of the system. Our work also contributes to clarify conditions for the experimental obser-

vation of SL, as discussed at the end of the article.

To understand the nature of SL it is essential to note that the fixed point corresponding to the DB state into which the initial condition collapses does not undergo a bifurcation itself. On the contrary, using standard methods [31–34] the bright breather fixed point can easily be numerically found to exist and to be linearly stable for *all* positive nonlinearity strengths. Linear stability analysis therefore does not suffice to understand the SL transition. The underlying idea of our approach is that near the SL threshold a single strong, localized fluctuation of the number of atoms locally brings the system’s state into the basin of attraction of a DB fixed point in phase space. The role of dissipation at this point is that DBs are attractors in dissipative systems [35–37], while Hamiltonian systems do not have attractors. In the simplest and most likely event a strong increase in the number of atoms happens on a single site that will become the center of the DB to be formed.

We therefore study first, how a single site excitation can lead to the formation of a DB and find that there exists a distinct nonlinearity strength at which this initial condition crosses over into a self-trapped state. We show that the origin of this *ST crossover* is an energy threshold describing the stability of self-trapped states (called the Peierls-Nabarro (PN) energy barrier [22, 38, 39]). Secondly, we statistically estimate the critical nonlinearity at the onset of SL by studying the probability that a fluctuation in a diffusive state exceeds this ST crossover and leads to the formation of a breather. The ST crossover and SL should not only be observable for BECs but as well, e.g., in coupled nonlinear optical waveguides [29, 40].

Consider the Bose-Hubbard Hamiltonian in the mean-field description [41, 42]

$$H = U \sum_{i=n}^M |\psi_n|^4 - \frac{J}{2} \sum_{n=1}^{M-1} (\psi_n^* \psi_{n+1} + \text{c.c.}) \quad (1)$$

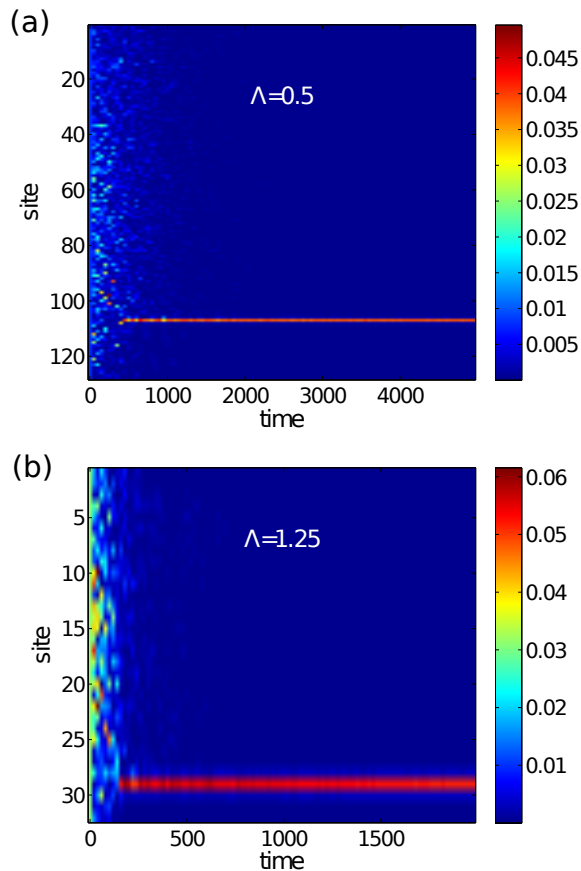


Figure 1: Demonstration of self-localization in a lattice with (a) $M = 128$ and (b) $M = 32$ sites based upon the dissipative DNLS. The color code shows $|\psi_n(t)|^2$ (normalized to 1 at $t = 0$). Time is measured in units of the tunneling rate J . The initial condition is a homogeneously populated lattice (i.e., constant norms) with random phases at each site uniformly drawn from $[0, 2\pi]$. Boundary dissipation rate at sites 1 and M is $\gamma = 0.2$. (a) The dissipative dynamics leads to formation of a discrete breather centered at site 107. The effective nonlinearity $\Lambda = L/M$ is $\Lambda = 0.5$ just above the self-localization threshold $\Lambda_b = 0.58$ (see Eq. 17). (b) A discrete breather forms centered at site 29. The effective nonlinearity is $\Lambda = 1.25$. In both panels, Λ is larger than the self-localization threshold Λ_b (cf. Eq. 17). Note that though the discrete breathers are more likely to form near the middle of the lattice, they can also emerge near the boundaries, as shown here.

with on-site interaction U , tunneling rate J , lattice index $n = 1 \dots M$, where M denotes the number of lattice sites. Including boundary dissipation, the mean-field equations of motion are given by the dissipative DNLS (see [6, 7, 43] for a derivation of the loss term)

$$i\dot{\psi}_n = L|\psi_n|^2\psi_n - \frac{1}{2}(\psi_{n-1} + \psi_{n+1}) - i\gamma\psi_n(\delta_{n,1} + \delta_{n,M}) \quad (2)$$

with $\hbar = 1$, nonlinearity $L = (2U/J)\mathcal{N}$, dissipation rate γ , total number of atoms \mathcal{N} and the normalization

$\sum_n |\psi_n|^2 = 1$. We introduce a measure of the *local nonlinearity* $L_n^{\text{local}} = (2UN/J)\mathcal{N}_n$, where $\mathcal{N}_n = |\psi_n|^2$ is the relative number of atoms (also referred to as the norm) at site n .

II. SELF-LOCALIZATION VS. SELF-TRAPPING

Though SL is based upon ST, it is distinguished by the way in which a stable (or metastable) and spatially localized state is reached. There are several ways to obtain self-trapping of BECs in optical lattices which we classify into three types.

Type I (*'static preparation'*): The quantum system is prepared in (or sufficiently close to) a self-trapped state. This has been realized in various experiments [11, 14, 15, 44]. Using a variational approach, a phase diagram has been calculated, that describes the transition from diffusion to ST for an initial Gaussian wave packet [19, 20], which, however, does not account for SL. Note that recent numerics for the DNLS [27] rather contradicts the phase diagram in [19].

Type II (*'dynamical preparation'*): Another route to ST is to apply a strong local dissipation pulse, which can depopulate one or more sites and create a stable isolated peak or vacancy [4, 6, 7, 23] (leading to the formation of a bright or dark breather). In particular, spatially resolved dissipative manipulation in an optical lattice using an electron beam with single-site addressability has been demonstrated [4].

Type III (*'self-localization'*): A third way to generate self-trapping is SL, where the system prepared in a random (generic) state in the presence of boundary or other local dissipation dynamically forms one or more DBs, see Figs. 1 and 2. In contrast to Type II, the positions where DBs form are not determined by the location of the leak [24–27]. In absence of boundary or local dissipation SL does not take place, see Fig. 2(b) and [24]. Also, below a threshold Λ_b , self-localization does not occur (cf. Fig. 2(c)). This threshold to SL has been observed in detail in ref. [45], in particular for lattices with large number of wells ($M = 128$ to $M = 4096$). A main purpose of this article is to derive an explicit formula for the SL threshold Λ_b (cf. Eq. 17).

III. SELF-TRAPPING CROSSOVER

Let us first consider the dissipationless case (which belongs to type I) with the following initial condition, where all atoms are located at site c , given by

$$\psi_n(t=0) = \delta_{nc}. \quad (3)$$

In which range of the nonlinearity will the majority of the atomic population stay self-trapped near site c (resulting in the formation of a DB)? In Fig. 3 the evolution of the particle density is shown. For $L = 1.6$ (Fig. 3(a))

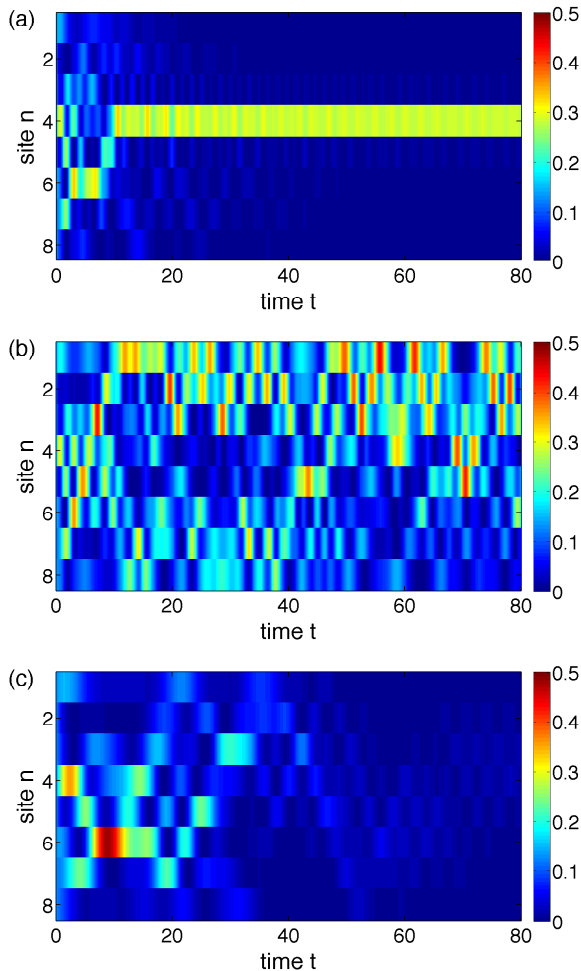


Figure 2: Self-localization can also be observed in small lattices, shown here for $M = 8$ wells (similar to the experimental setup in [46]) for the DNLS with boundary dissipation rate $\gamma = 0.2$. The color code shows the atomic density $|\psi_n(t)|^2$. Initial condition is a homogeneously populated lattice with random phases as in Fig. 1. Three representative cases with identical initial condition are shown, SL is observed only in panel (a). Time is measured in units of J , i.e. for $J = 10\text{Hz}$, which is a typical experimental value in [46], the discrete breather in (a) forms around time $t = 1\text{s}$. **(a)** Self-localization with $\Lambda = 1.354 = 1.5\Lambda_b$. **(b)** Without dissipation ($\gamma = 0$) no self-localization takes place. For times $t \gtrsim 5/J$, the plot strongly differs qualitatively from the dissipative case (a). We carefully checked for different parameter regimes M and Λ , that even for times several orders of magnitude longer than depicted here, SL does not occur for $\gamma = 0$. **(c)** For the dissipative case where $\Lambda = 0.5 < \Lambda_b$, no self-localization takes place and the number of atoms in the lattice decays quickly.

the particle density initially decays exponentially in time and then populates the whole lattice evenly. In contrast, a completely different behavior is observed for $L = 2.4$ in Fig. 3(b), where the initial condition relaxes into a ST state which is exponentially localized in space. A necessary condition for ST is $L_n^{\text{local}} > L_{\text{co}}$, where L_{co} is the

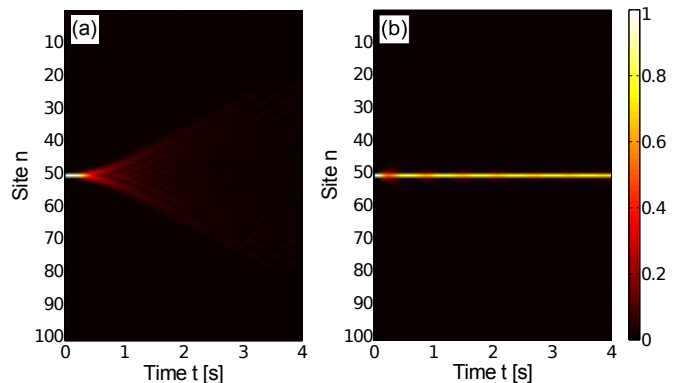


Figure 3: A ST crossover for a δ -like initial condition, where all atoms are located at a single site c , is found both beyond and within the mean-field description (depicted here for the DNLS). The color code shows the normalized atomic density $|\psi_n(t)|^2$. **(a)** Below the crossover, for $L = 1.6 < L_{\text{co}}$, the localized peak at $t = 0$ decays exponentially fast. **(b)** Above the crossover (shown is $L = 2.4 > L_{\text{co}}$) a discrete breather forms. The particle density is stable and decays exponentially in space away from the center. About 85% of the atoms are located in three sites after time $t = 4\text{s}$. Other parameters are $M = 101$, $c = 51$, $J = 10\text{Hz}$ and $\gamma = 0$.

value of the nonlinearity at the *crossover* that separates the diffusive from the ST regime. We define that ST is encountered, if $\min |\psi_c(t > T)|^2 > a$ for large T , which is independent of T once a breather has formed. The value for a can be estimated via the position of a saddle point (in the so-called Peierls-Nabarro energy landscape of a local trimer model, see below) that dictates the stability of the DB [22], which is shown in Fig. 4(a). In the limit $L \rightarrow \infty$ the saddle point is found analytically at $N_2 = 1/2$ [22], we therefore estimate $a = 1/2$. Starting with initial condition (3) and choosing $T = 1\text{s}$, the crossover from diffusion to ST is numerically found to be at $L_{\text{co}}^{\text{num}} = 2.2463$. Integration times were at least $10T$.

In the following, we will examine the observed ST crossover in detail, for which we make use of a general concept called the PN energy barrier. It is given by the energy difference $|E_b - E_e|$, where E_b is the total energy of a DB centered at a single lattice site and E_e is the energy of a more extended breather centered between two lattice sites [38, 39]. The PN barrier is based on the notion, that due to continuity, the process of translating a localized object with energy E_b from one lattice site to the adjacent one involves an intermediate state with different energy E_e .

We will connect the ST crossover to the stability of a DB. It has been shown that the stability of a DB can be well-described via a reduced problem of only few degrees of freedom [29], which reflects the fact that the breather is highly (exponentially) localized. This ‘local Ansatz’ has been further developed analytically in a local trimer (which is a subsystem consisting of three sites) on the so-called PN energy landscape [22], which is defined by $H_{\text{PN}} = \max_{\delta\phi_{ij}}(H)$, with $\psi_n = \sqrt{N_n} \exp(i\phi_n)$ and

$\delta\phi_{ij} = \phi_i - \phi_j$ [61]. The PN landscape reads [22]

$$H_{\text{PN}} = \frac{L}{2}(N_1^2 + N_2^2 + N_3^2) + (\sqrt{N_1} + \sqrt{N_3})\sqrt{N_2}. \quad (4)$$

Figure 4(a) shows the PN landscape of the trimer at the ST crossover. The bright DB, which is linearly stable [47], is located in the top ‘eye’ of the energy landscape. The two saddle points just below $N_2 = 1/2$ (related to a migration of the DB from site 2 to site 1 and 3 respectively) are connected to the PN barrier and the total energy threshold dictating the breather stability is given by [22]

$$E_{\text{PN}}(L) = \frac{L}{4} + \frac{1}{2} + \frac{1}{4L} - \frac{1}{4L^2} + \frac{1}{4L^3} - \frac{9}{16L^4} + \mathcal{O}\left(\frac{1}{L^5}\right). \quad (5)$$

The energy of a bright breather E_b is a maximum of the total energy E of the trimer. As long as the total energy of the local trimer $E_{\text{PN}} < E \leq E_b$ is above the threshold, a breather remains pinned to a lattice site. The total energy for the initial condition (3) reads $E(L) = L/2$, which can be seen directly from Eq. (1) as the energy is measured in units of the tunneling rate J (cf. Eq. (2)). Hence, the crossover L_{co} is reached, when E_{PN} (Eq. (5)) is equal to $L/2$, and we obtain

$$L_{\text{co}}^5 - 2L_{\text{co}}^4 - L_{\text{co}}^3 + L_{\text{co}}^2 - L_{\text{co}} + \frac{9}{4} = 0. \quad (6)$$

We find $L_{\text{co}} = 2.2469$, in excellent agreement with the numerical value. This result means that the ST crossover, which is observed in a one-dimensional optical lattice, can be described with high degree of accuracy by the PN barrier of a local trimer. Given that the PN barrier describes the stability of self-trapped states in a very broad context, we expect that the three different types to obtain ST (static, dynamical and self-localized) in discrete systems eventually are related to the PN barrier.

The general behavior near the ST crossover is depicted in Fig. 4(b). The PN barrier bends off the total energy line for increasing $L > L_{\text{co}}$, which leads to a growing area of stability (given by $E_0(L) > E_{\text{PN}}(L)$). In the limit $L \rightarrow \infty$, the initial total energy E_0 (red line) asymptotically approaches the total energy E_b of the bright breather (blue thick line) [62]. The exact breather energy $E_b(L)$, here for $M = 101$ sites can be calculated numerically using standard methods (such as the anti-continuous limit [29, 32, 48]), while we applied a different iterative approach [34].

A. Generalized BBR method

To study, how the ST crossover manifests beyond the mean-field description, we use the Bogoliubov Backreaction (BBR) method [49, 50], which includes higher-order correlation functions and allows a consistent calculation of the condensate fraction of the BEC. The BBR

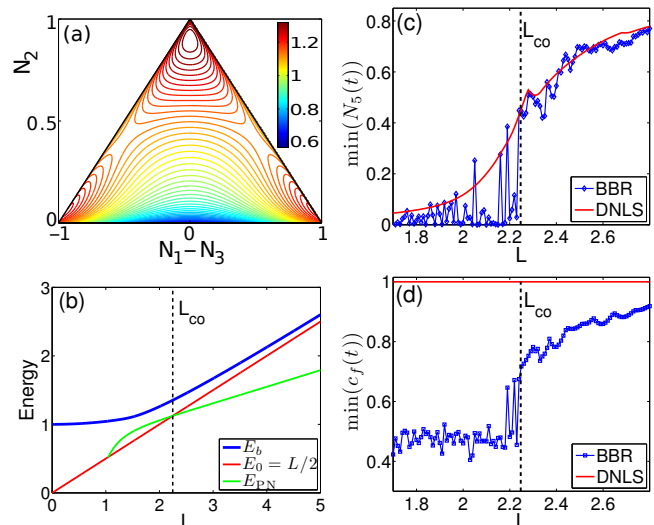


Figure 4: (a) The PN energy landscape H_{PN} exhibits a bright DB (located in the top ‘eye’ on the PN landscape at $N_2 = 0.902$ and $N_1 = N_3 = 0.049$) and two degenerate saddle points that mark the boundary of stability of the DB. The color code shows the PN landscape (Eq. (4)) for $L = L_{\text{co}} = 2.2469$. (b) The ST crossover is found at the crossing (dashed line) of the total energy $E_0 = L/2$ (red line) with the PN energy barrier E_{PN} (Eq. (5), green line). The corresponding energy at the crossing is the total energy of the saddle points shown in (a). For $L \rightarrow \infty$, E_0 asymptotically approaches the total energy of the bright breather E_b (blue line). (c-d) Including quantum corrections using the BBR method (blue line), the ST crossover exhibits a much sharper transition compared to the mean-field result (red line), here shown for $M = 9$ sites. We report the minimum number of atoms at the central site $\min(N_5)$ and the condensate fraction $\min(c_f(t))$. The dashed line in (c-d) marks the crossover at L_{co} for an infinite lattice. Other parameters are $\gamma = 0.5$ Hz, $N = 200$ atoms, $J = 10$ Hz. The minima were determined in the interval $t \in [0.25, 0.5]$ s.

method has recently been generalized to the dissipative case [6, 7], which is crucial for our study. The generalized BBR method is especially useful if the many-body state is close to, but not exactly equal to a pure BEC, in particular it accurately predicts the onset of a depletion of the condensate mode [6].

We shortly review the main steps of the derivation of the generalized BBR method and point out its validity. The coherent dynamics of ultracold atoms in deep optical lattices is described by the Bose-Hubbard Hamiltonian

$$\hat{H} = -J \sum_j \left(\hat{a}_{j+1}^\dagger \hat{a}_j + \hat{a}_j^\dagger \hat{a}_{j+1} \right) + \frac{U}{2} \sum_j \hat{a}_j^\dagger \hat{a}_j^\dagger \hat{a}_j \hat{a}_j, \quad (7)$$

where \hat{a}_j and \hat{a}_j^\dagger are the bosonic annihilation and creation operators, J denotes the tunneling rate between the wells and U is the on-site interaction. The BHH is obtained when the lattice is sufficiently deep, such that the dynamics is restricted to the lowest Bloch band. We measure energy in frequency units by setting $\hbar = 1$.

To consider the quantum dynamics in presence of dissipation, we use a master equation in Lindblad form [51]

$$\dot{\hat{\rho}} = -i[\hat{H}, \hat{\rho}] + \mathcal{L}\hat{\rho}. \quad (8)$$

Localized particle loss and phase noise are described by the Liouvillians [51]

$$\mathcal{L}_{\text{loss}}\hat{\rho} = -\frac{1}{2} \sum_j \gamma_j \left(\hat{a}_j^\dagger \hat{a}_j \hat{\rho} + \hat{\rho} \hat{a}_j^\dagger \hat{a}_j - 2\hat{a}_j \hat{\rho} \hat{a}_j^\dagger \right), \quad (9)$$

$$\mathcal{L}_{\text{phase}}\hat{\rho} = -\frac{\kappa}{2} \sum_j \hat{n}_j^2 \hat{\rho} + \hat{\rho} \hat{n}_j^2 - 2\hat{n}_j \hat{\rho} \hat{n}_j, \quad (10)$$

where γ_j denotes the particle loss rate at site j and κ is the strength of the phase noise.

In this article, we set $\kappa = 0$, thus considering only particle loss. For the purpose of generality, the terms resulting from phase noise are included below.

We will first derive the mean-field equations from this – so far exact – approach. The higher order correlation functions that are the building block of the BBR method will then appear naturally. We start from the single particle reduced density matrix (SPDM) $\sigma_{jk} = \langle \hat{a}_j^\dagger \hat{a}_k \rangle = \text{tr}(\hat{a}_j^\dagger \hat{a}_k \hat{\rho})$ [49, 50, 52, 53]. The equations of motion for σ_{jk} are obtained from the master equation (8)

$$\begin{aligned} i \frac{d}{dt} \sigma_{j,k} &= \text{tr} \left(\hat{a}_j^\dagger \hat{a}_k [\hat{H}, \hat{\rho}] + i \hat{a}_j^\dagger \hat{a}_k \mathcal{L} \hat{\rho} \right) \\ &= -J(\sigma_{j,k+1} + \sigma_{j,k-1} - \sigma_{j+1,k} - \sigma_{j-1,k}) \\ &\quad + U(\sigma_{kk}\sigma_{jk} + \Delta_{kkjk} - \sigma_{jj}\sigma_{jk} - \Delta_{jjjk}), \\ &\quad -i \frac{\gamma_j + \gamma_k}{2} \sigma_{j,k} - i\kappa(1 - \delta_{j,k})\sigma_{j,k}, \end{aligned} \quad (11)$$

with the variances $\Delta_{jk\ell m} = \langle \hat{a}_j^\dagger \hat{a}_k \hat{a}_\ell^\dagger \hat{a}_m \rangle - \langle \hat{a}_j^\dagger \hat{a}_k \rangle \langle \hat{a}_\ell^\dagger \hat{a}_m \rangle$. In the mean-field limit $N \rightarrow \infty$ (where UN remains finite), one can neglect the variances $\Delta_{jk\ell m}$ in Eq. (11) in order to obtain a closed set of evolution equations. This is the case for a pure BEC, as the variances scale only linearly with the particle number N , while the products $\sigma_{jk}\sigma_{\ell m}$ scale as N^2 .

To describe many-body effects such as quantum correlations and the depletion of the condensate for large, but finite particle numbers, we explicitly take the variances $\Delta_{jk\ell m}$ into account. The time evolution of the variances $\Delta_{jk\ell m}$ includes six-point correlation functions $\langle \hat{a}_j^\dagger \hat{a}_m \hat{a}_k^\dagger \hat{a}_n \hat{a}_r^\dagger \hat{a}_s \rangle$. And the equations of motion for the six-point function then contain even higher correlation functions and so on. In order to obtain a closed set of equations of motion, the higher-order (six-point) correlation functions are truncated as follows [50]:

$$\begin{aligned} \langle \hat{a}_j^\dagger \hat{a}_m \hat{a}_k^\dagger \hat{a}_n \hat{a}_r^\dagger \hat{a}_s \rangle &\approx \langle \hat{a}_j^\dagger \hat{a}_m \hat{a}_k^\dagger \hat{a}_n \rangle \langle \hat{a}_r^\dagger \hat{a}_s \rangle \\ &\quad + \langle \hat{a}_j^\dagger \hat{a}_m \hat{a}_r^\dagger \hat{a}_s \rangle \langle \hat{a}_k^\dagger \hat{a}_n \rangle + \langle \hat{a}_k^\dagger \hat{a}_n \hat{a}_r^\dagger \hat{a}_s \rangle \langle \hat{a}_j^\dagger \hat{a}_m \rangle \\ &\quad - 2\langle \hat{a}_j^\dagger \hat{a}_m \rangle \langle \hat{a}_k^\dagger \hat{a}_n \rangle \langle \hat{a}_r^\dagger \hat{a}_s \rangle. \end{aligned} \quad (12)$$

Within this framework, we see that the mean-field approximation results from truncating the four-point correlation functions (and thus neglecting the variances $\Delta_{jk\ell m}$), while within the BBR approach the four-point functions are taken explicitly into account and the six-point functions are truncated. With this ansatz we obtain the generalized BBR equations of motion (see [6, 7] for details). The relative error induced by the truncation vanishes as $1/N^2$ with increasing particle number. Close to a pure condensate, the BBR method thus provides a much more accurate description of the many-body dynamics than the simple mean-field approximation.

B. ST crossover beyond mean-field

In Fig. 4(c) the minimum remaining number of atoms (normalized to 1) at the central site are shown for $M = 9$ sites and initial condition (3) using the generalized BBR method and compared to the mean-field result. Boundary dissipation was applied in both cases, reducing reflections from the edges of the lattice. The condensate fraction c_f is the fraction of the number of condensed atoms and is given by the largest eigenvalue of the SPDM $\sigma_{j,k}$, whereas the total number of atoms is given by the trace of $\sigma_{j,k}$ [49, 52, 54].

The crossover at L_{co} (dashed line in Fig. 4(c-d)), which we have derived in Eq. 6, is in excellent agreement with the BBR calculations. By including quantum corrections, the ST crossover becomes much sharper which is also reflected by a jump in the condensate fraction, see the blue curve in Fig. 4(d), where we report $\min(c_f(t))$ for times $t \in [0.25, 0.5]$ s. In contrast, the mean-field dynamics based upon the DNLS per se assumes a pure BEC, i.e., $c_f = 1$ (red line).

While stable motion above the crossover allows for long-time coherence, unstable motion below the crossover leads to depletion of the condensate [55]. A profound understanding of the ST crossover therefore might be viable for controlled quantum state preparation using spatially localized initial conditions, such as Eq. (3).

IV. SELF-LOCALIZATION

We now turn our focus to SL, where the dynamics finds self-trapped states by itself in presence of weak boundary dissipation [24–27], resembling a phase transition [26]. To consistently investigate the dynamics in different lattices sizes M , we require the initial density $\rho = \mathcal{N}/M$ to be constant. Rescaling L accordingly results in an effective nonlinearity $\Lambda = L/M$ [26]. Starting with a homogeneous initial condition with equal norm on all lattice sites and random phases, the transition to SL has been observed at a critical interaction strength Λ_b for which we will derive an explicit expression in the following. The condition for self-trapping reads $L_n^{\text{local}} = LN_n = \Lambda MN_n > L_{\text{co}}$. The critical nonlinearity Λ_b for the dynamical formation of a

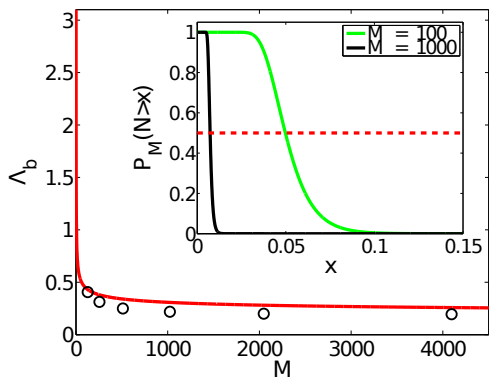


Figure 5: The SL transition at Λ_b (red line) given by Eq. (17) is an upper bound numerical results. The data (black circles) was extracted for boundary dissipation rate $\gamma = 0.2$ Hz from Fig. 1 in [26], where a sharp drop of the ‘participation ratio’ clearly marks the SL transition. The inset shows the probability for detecting a norm x (Eq. (15)) which exhibits a sharp transition and becomes a step function in the limit $M \rightarrow \infty$.

breather is obtained for $L_n^{\text{local}} = L_{\text{co}}$, hence we find

$$\Lambda_b = \frac{L_{\text{co}}}{MN_m}. \quad (13)$$

As the only unknown quantity in Eq. (13) is the maximum single site norm N_m , calculating Λ_b is reduced to a very general question: What is the probability to find a site with norm larger than a given value N in the optical lattice? In the diffusive regime, the probability distribution of norms x in the lattice is $w(x) = M \exp(-Mx)$ [26]. The probability that the norm at a certain site is smaller than x is

$$P(N < x) = \int_0^x w(x') dx' = 1 - e^{-Mx}. \quad (14)$$

Assuming that the populations at the M sites are independent from each other, the probability that at least one site has a norm larger than x reads

$$P_M(N > x) = 1 - [1 - e^{-Mx}]^M, \quad (15)$$

which approaches a step function for $M \rightarrow \infty$ (see inset of Fig. 5). Thus, the largest norm that is found in the diffusive regime is given for large M by $P_M(N > x) \approx 1/2$ (red dashed line in Fig. 5). Insertion into Eq. (15) yields

$$N_m \equiv x = \ln\left[\frac{1}{1 - (1/2)^{1/M}}\right]/M. \quad (16)$$

With Eq. 13 the SL transition is found to be at the critical nonlinearity

$$\Lambda_b = \frac{L_{\text{co}}}{\ln\left[\frac{1}{1 - (1/2)^{1/M}}\right]}, \quad (17)$$

which is shown in Fig. 5 (red line). As in deriving Eq. (16) it was assumed that the populations at the M sites are independent, we have effectively calculated an upper bound to Λ_b , in excellent agreement with the numerical results in [26] (shown as black circles in Fig. 5).

V. EXPERIMENTAL REALIZATION

We expect that the ST crossover can be readily studied in present experiments [4, 56, 57]. The initial condition (3) relates to a BEC cloud at a single lattice site, while the interatomic interaction can be tuned via a Feshbach resonance. In contrast, observing SL in optical lattices is more delicate. A prerequisite to observe SL is dissipation.

While discrete breathers exist as well in Hamiltonian systems [29, 30], they become attractors of the dynamics in dissipative systems [35–37] which is crucial for SL. Furthermore, local dissipation helps stabilizing once formed DBs by damping down phonons in the lattice.

Local dissipation has been realized with single site resolution using a focused electron beam [4, 57], while another possibility is to apply a microwave field to locally spin flip atoms inside the BEC [58, 59]. The experiment, however, needs to allow for sufficient propagation time so that SL can form, in the course of which chaotic dynamics and dynamical instabilities typically lead to depletion of the condensate [44, 55, 60]. A remedy could be to reduce the timescale by considering lattices with few number of wells (as in Fig. 2) or to prepare an initial condition, that has more than exponentially small probability for high norms.

VI. CONCLUSION

In conclusion, we analyzed the nature of SL in optical lattices, which previously has been observed phenomenologically in several studies [24–27], explaining recent numerical findings [26]. SL represents an alternative way to induce localization where the preparation of initial wave packets is not necessary.

Our results show that the SL transition at Λ_b for which we derived an explicit estimate (Eq. (17)) is based upon two constituent parts. The first part is a ST crossover, which we studied both within and beyond the mean-field description. The second part is based on the probability, that the dynamics leads to a local energy above the PN energy barrier.

Given the simplicity of initial condition (3) used to probe the ST crossover, we expect that the crossover is not only experimentally readily accessible, but that its understanding could also be vital in generating long-time coherent states, without the need to fine-tune the initial state.

Acknowledgments

We thank David K. Campbell, Dirk Witthaut, Jérôme Dornignac and Thomas Neff for useful discussions. We

acknowledge financial support by the German Research Foundation (DFG, grant no. HE 6312/1-1 and Forschergruppe 760).

-
- [1] S. Diehl, A. Micheli, A. Kantian, B. Kraus, H. P. Büchler, and P. Zoller, *Nat. Phys.* **4**, 878 (2008).
- [2] B. Kraus, H. Büchler, S. Diehl, A. Kantian, A. Micheli, and P. Zoller, *Phys. Rev. A* **78**, 042307 (2008).
- [3] F. Verstraete, M. M. Wolf, and J. I. Cirac, *Nat. Phys.* **5**, 633 (2009).
- [4] T. Gericke, P. Würtz, D. Reitz, T. Langen, and H. Ott, *Nat. Phys.* **4**, 949 (2008).
- [5] E. Graefe, H. J. Korsch, and A. Niederle, *Phys. Rev. Lett.* **101**, 150408 (2008).
- [6] D. Witthaut, F. Trimborn, H. Hennig, G. Kordas, T. Geisel, and S. Wimberger, *Phys. Rev. A* **83**, 063608 (2011).
- [7] F. Trimborn, D. Witthaut, H. Hennig, G. Kordas, T. Geisel, and S. Wimberger, *Eur. Phys. J. D* **63**, 63 (2011).
- [8] S. Burger, K. Bongs, S. Dettmer, and W. Ertmer, *Phys. Rev. Lett.* (1999).
- [9] L. Khaykovich, F. Schreck, G. Ferrari, T. Bourdel, J. Cubizolles, L. D. Carr, Y. Castin, and C. Salomon, *Science* **296**, 1290 (2002).
- [10] K. Strecker, G. Partridge, A. Truscott, and R. Hulet, *Nature* **417**, 150 (2002).
- [11] B. Eiermann, T. Anker, M. Albiez, M. Taglieber, P. Treutlein, K.-P. Marzlin, and M. K. Oberthaler, *Phys. Rev. Lett.* **92**, 230401 (2004).
- [12] S. Cornish, S. Thompson, and C. Wieman, *Phys. Rev. Lett.* **96**, 170401 (2006).
- [13] S. Stellmer, C. Becker, P. Soltan-Panahi, E.-M. Richter, S. Dörscher, M. Baumert, J. Kronjäger, K. Bongs, and K. Sengstock, *Phys. Rev. Lett.* **101**, 120406 (2008).
- [14] M. Albiez, R. Gati, J. Fölling, S. Hunsmann, M. Cristiani, and M. Oberthaler, *Phys. Rev. Lett.* **95**, 010402 (2005).
- [15] T. Zibold, E. Nicklas, C. Gross, and M. Oberthaler, *Phys. Rev. Lett.* **105**, 204101 (2010).
- [16] K. Ø. Rasmussen, S. Aubry, A. R. Bishop, and G. Tsironis, *Eur. Phys. J. B* **15**, 169 (2000).
- [17] K. Rasmussen, T. Cretegny, P. Kevrekidis, and N. Gronbach-Jensen, *Phys. Rev. Lett.* **84**, 3740 (2000).
- [18] S. Raghavan, A. Smerzi, S. Fantoni, and S. R. Shenoy, *Phys. Rev. A* **59**, 620 (1999).
- [19] A. Trombettoni and A. Smerzi, *Phys. Rev. Lett.* **86**, 2353 (2001).
- [20] A. Trombettoni and A. Smerzi, *J. Phys. B* **34**, 4711 (2001).
- [21] A. Smerzi, S. Fantoni, S. Giovanazzi, and S. Shenoy, *Phys. Rev. Lett.* **79**, 4950 (1997).
- [22] H. Hennig, J. Dornignac, and D. Campbell, *Phys. Rev. A* **82**, 053604 (2010).
- [23] D. Witthaut, F. Trimborn, and S. Wimberger, *Phys. Rev. Lett.* **101**, 200402 (2008).
- [24] R. Livi, R. Franzosi, and G.-L. Oppo, *Phys. Rev. Lett.* **97**, 060401 (2006).
- [25] R. Franzosi, R. Livi, and G.-L. Oppo, *J. Phys. B* **40**, 1195 (2007).
- [26] G. S. Ng, H. Hennig, R. Fleischmann, T. Kottos, and T. Geisel, *New J. Phys.* **11**, 073045 (2009).
- [27] R. Franzosi, R. Livi, G. Oppo, and A. Politi, *Nonlinearity* **24**, R89 (2011).
- [28] R. Franzosi, S. Giampaolo, and F. Illuminati, *Phys. Rev. A* **82**, 063620 (2010).
- [29] S. Flach and A. V. Gorbach, *Phys. Rep.* **467**, 1 (2008).
- [30] D. K. Campbell, S. Flach, and Y. S. Kivshar, *Phys. Today* **57**, 43 (2004).
- [31] J. Carr and J. C. Eilbeck, *Phys. Lett. A* **109A**, 201 (1985).
- [32] S. Aubry, *Physica D* **103**, 201 (1997).
- [33] S. Darmanyan, A. Kobayakov, and F. Lederer, *J. Exp. Theor. Phys.* **86**, 682 (1998).
- [34] L. Proville and S. Aubry, *Eur. Phys. J. B* **11**, 41 (1999).
- [35] S. Flach and C. R. Willis, *Physics Reports* **295**, 181 (1998).
- [36] P. J. Martinez, M. Meister, L. M. Floria, and F. Falo, *Chaos* **13**, 610 (2003).
- [37] R. S. MacKay and J. A. Sepulchre, *Physica D: Nonlinear Phenomena* **119**, 148 (1998).
- [38] Y. S. Kivshar and D. K. Campbell, *Phys. Rev. E* **48**, 3077 (1993).
- [39] B. Rumpf, *Phys. Rev. E* **70**, 016609 (2004).
- [40] D. N. Christodoulides, F. Lederer, and Y. Silberberg, *Nature* **424**, 817 (2003).
- [41] C. J. Pethick and H. Smith, *Bose-Einstein Condensation in Dilute Gases* (Cambridge University Press, Cambridge, UK, 2008).
- [42] P. Buonsante and V. Penna, *J. Phys. A* **41**, 175301 (2008).
- [43] J. Jeffers, P. Horak, S. Barnett, C. Baxter, and P. Radmore, *Phys. Rev. A* **62**, 043602 (2000).
- [44] I. Bloch, *Nat. Phys.* **1**, 23 (2005).
- [45] G. S. Ng, H. Hennig, R. Fleischmann, T. Kottos, and T. Geisel, *Arxiv preprint arXiv:0805.1948* (2008).
- [46] J. Estève, C. Gross, A. Weller, S. Giovanazzi, and M. K. Oberthaler, *Nature* **455**, 1216 (2008).
- [47] P. Buonsante, R. Franzosi, and V. Penna, *Phys. Rev. Lett.* **90**, 050404 (2003).
- [48] J. Marin and S. Aubry, *Nonlinearity* **9**, 1501 (1996).
- [49] A. Vardi and J. Anglin, *Phys. Rev. Lett.* **86**, 568 (2001).
- [50] I. Tikhonenkov, J. Anglin, and A. Vardi, *Phys. Rev. A* **75**, 013613 (2007).
- [51] H.-P. Breuer and F. Petruccione, p. 625 (2002).
- [52] J. Anglin and A. Vardi, *Phys. Rev. A* **64**, 013605 (2001).
- [53] F. Trimborn, D. Witthaut, and H. J. Korsch, *Phys. Rev. A* **77**, 043631 (2008).
- [54] A. Leggett, *Rev. Mod. Phys.* (2001).
- [55] Y. Castin and R. Dum, *Phys. Rev. Lett.* **79**, 3553 (1997).
- [56] T. Anker, M. Albiez, R. Gati, S. Hunsmann, B. Eiermann, A. Trombettoni, and M. Oberthaler, *Phys. Rev. Lett.* **94**, 8451 (2005).
- [57] P. Würtz, T. Langen, T. Gericke, A. Koglbauer, and

- H. Ott, Phys. Rev. Lett. **103**, 080404 (2009).
- [58] I. Bloch, T. Hänsch, and T. Esslinger, Phys. Rev. Lett. **82**, 3008 (1999).
- [59] A. Öttl, S. Ritter, M. Köhl, and T. Esslinger, Phys. Rev. Lett. **95**, 090404 (2005).
- [60] L. Fallani, L. De Sarlo, J. Lye, M. Modugno, R. Saers, C. Fort, and M. Inguscio, Phys. Rev. Lett. **93**, 140406 (2004).
- [61] In ref. [22] ($-H_{\text{PN}}$) is called the *lower* PN landscape due to the additional minus sign. A second energy landscape is obtained via $H_{\text{PN}}^* = \min_{\delta\phi_{ij}}(H)$, however, to study the ST crossover it is sufficient to consider only H_{PN} .
- [62] For $L \ll 1$ the stability of a bright breather is not described by Eq. (5) [22].